Paper Number 07ATC-104

REDUCING CORROSION FATIGUE AND SCC FAILURES IN 300M STEEL LANDING GEAR USING LOW PLASTICITY BURNISHING

Doug Hornbach and Paul Prevéy
Lambda Technologies

ABSTRACT

300M steel is often used in landing gear because of its high strength and high fracture toughness. Conversely, 300M steel is highly susceptible to corrosion fatigue and stress corrosion cracking (SCC), which can lead to catastrophic consequences for aircraft landing gear. Shot peening and plating of the landing gear are used to suppress corrosion fatigue and SCC with limited success. A method that will produce deeper compression in critical regions of landing gear will provide a dramatic improvement in foreign object damage (FOD) tolerance, corrosion fatigue strength and SCC susceptibility. This paper discusses the use of low plasticity burnishing (LPB) to provide a deep layer of residual compression to improve damage tolerance and mitigate SCC of 300M steel.

The fatigue performance of LPB processed 300M steel test samples were compared to those in a shot peened or low-stress-ground (LSG) condition. LPB treatment dramatically improved the high cycle fatigue (HCF) and corrosion fatigue performance with and without a simulated defect. LPB reduced the surface stress well below the SCC threshold for 300M, even under high tensile applied loads, effectively suppressing the SCC failure mechanism. SCC testing of LPB treated landing gear sections at tensile stresses ranging from 1030 to 2270 MPa (150 to 180 ksi) was terminated after 1500 hrs without failure, compared to failure in as little as 13 hours without LPB treatment.

INTRODUCTION

SCC, corrosion fatigue, and FOD can dramatically reduce the life of aircraft landing gear components. Ultrahigh strength steels such as 4340, AF1410, and 300M are commonly used for landing gear components where a combination of high strength and fracture toughness is needed. Most of these ultrahigh strength steels are prone to SCC and corrosion fatigue.[1-4]

Corrosion pits from salt spray exposure are common sites of fatigue crack initiation in high strength steel. Salt corrosion pitting occurs during exposure to a marine atmosphere and results in intergranular corrosion to a depth depending on the time of exposure, temperature, and the service environment. The pronounced fatigue strength reduction caused by salt pit corrosion is well established for steels[5] and typically reduces the endurance limit to approximately half of the uncorroded value.

The phenomenon of SCC is caused by a combination of susceptible material, corrosive environment, and tensile stress above a threshold, as illustrated in Figure 1. Solutions to reduce the susceptibility to corrosion and the environment have included modifying the material (alloy chemistry), or the use of protective coatings. Other alloys[2,3] like Aermet100, Custom250, Custom465, and Allvac240 have shown some improved resistance to SCC. Cadmium plating of the steel to retard corrosion and SCC have been standard practice for many landing gear systems.[4] In this paper, a novel approach of “mechanical suppression” of SCC and corrosion fatigue is presented. SCC is mitigated by introducing a layer of surface compression with LPB to maintain the net surface stress below the SCC threshold.

The use of compressive residual stresses in metallic components has long been recognized[6-9] to lead to enhanced fatigue strength. The fatigue strength of many engineering components is improved by shot peening (SP) or cold working, or as a by-product of a surface hardening treatment like carburizing/nitriding, physical vapor deposition, etc. Treatments like LPB[10], laser shock peening (LSP),[11] and ultrasonic peening[12] have emerged that benefit fatigue prone engineering components to different degrees. In all surface treatment processes, key benefits are obtained when deep compression is achieved with minimal cold work of the surface.

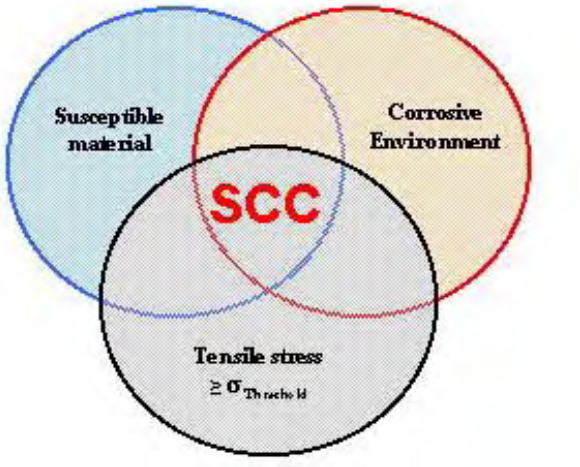

FIGURE 1 - SCC susceptibility diagram illustrating the need for the combination of a susceptible material, corrosive environment and threshold tensile stress to cause SCC.

LPB has been demonstrated to provide a deep surface layer of high magnitude compression in various aluminum, titanium, and nickel based alloys and steels. The deep compressive residual stress on the surface of these materials mitigates fatigue damage including FOD,[13-15] fretting,[16-17] and corrosion.[18-21] The LPB process can be performed on conventional CNC machine tools at costs and speeds comparable to conventional machining operations such as surface milling.

The intent of this program was to study the effect of a compressive surface residual stress state imparted by the LPB process upon the mechanisms of corrosion fatigue, damage tolerance and SCC in 300M steel. These results were compared to those obtained after a conventional SP surface treatment.

EXPERIMENTAL TECHNIQUE

MATERIAL AND HEAT TREAT

300M steel was procured in the form of 12.7 mm (0.5 in.) thick plates. Bars of nominal dimensions of 9.5 mm X 31.75 mm X 203.2 mm (0.375 in. X 1.25 in. X 8 in.) were machined and heat-treated. The nominal composition and tensile properties of the heat-treated steel are as follows:
0.2% Y.S. = 1,690 MPa (245 ksi), UTS = 2,000 MPa (290 ksi), Elong. = 10%, Hardness = 55 HRC

LPB PROCESSING

LPB process parameters were developed for thick sections of 300M steel using proprietary methods. The CNC control code was modified to allow positioning of the LPB tool in a series of passes along the gage section while controlling the burnishing pressure to develop the desired magnitude of compressive stress with relatively low cold working. Figure 2 shows a thick section fatigue specimen in the process of being LPB processed in the four-axis manipulator on the CNC milling machine.

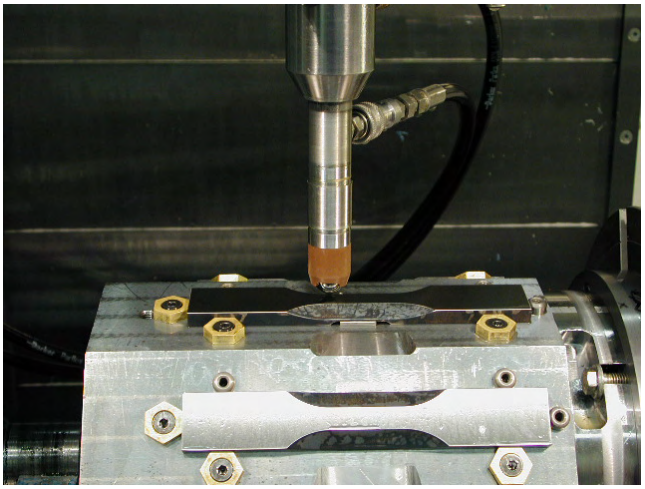

FIGURE 2 - A set of 8 thick section specimens being LPB processed in a 4-axis CNC milling machine.

SP PROCESSING

Shot peening was performed using a conventional air blast peening system equipped with a rotating table on two sets of fatigue specimens with the following process parameters: 150% coverage and CCW14 shot; both 8A and 10A intensities were used for purposes of residual stress measurement, while only SP specimens with 10A intensity were used for fatigue testing.

Residual Stress Measurement

X-ray diffraction residual stress measurements were made at the surface and at several depths below the surface on LPB treated fatigue specimens. Measurements were made in the longitudinal direction in the fatigue specimen gage employing a $\sin^2\psi$ technique and the diffraction of chromium Kα1 radiation from the (211) planes of steel. The lattice spacing was first verified to be a linear function of $\sin^2\psi$ as required for the plane stress linear elastic residual stress model.[22-25]

Material was removed electrolytically for subsurface measurement in order to minimize possible alteration of the subsurface residual stress distribution as a result of material removal. The residual stress measurements were corrected for both the penetration of the radiation into the subsurface stress gradient[26] and for stress relaxation caused by layer removal.[27]

The value of the x-ray elastic constants required to calculate the macroscopic residual stress from the strain normal to the (211) planes of steel were determined in accordance with ASTM E1426-9. Systematic errors were monitored per ASTM specification E915.

Residual stresses were measured in all surface treated specimens (both LPB processed and SP) before and after exposure to 400°F for 48 hours. The thermal treatment was selected to simulate an aggressive hydrogen bake-out used in landing gear production following cadmium or chromium plating, and allowed examination of any thermal relaxation of the compressive layer.

Fatigue and Stress Corrosion Testing

HCF tests were performed under constant amplitude loading on a Sonntag SF-1U fatigue machine at ambient temperature (~72F) in four-point bending mode. The cyclic frequency and stress ratio, R ($\sigma_{min}/\sigma_{max}$), were 30 Hz and 0.1 respectively. Corrosion fatigue testing was performed in neutral 3.5% NaCl salt solution prepared with de-ionized water. Filter papers were soaked with the solution, wrapped around the gage section of the fatigue test specimen, and sealed with a plastic film to avoid evaporation. Figure 3 shows a specimen with the salt solution soaked filter paper sealed around the gauge section.

FIGURE 3 - A thick section specimen with 3.5% salt solution soaked tissue wrapped around the gage section.

FOD was simulated with a semi-elliptical surface EDM notch as shown in Figure 4. Figure 5 shows the specimen mounted in the four-point bend fixture assembled for fatigue testing in a Sonntag SF-1U HCF machine. The following table describes the test conditions used in this study:

	Baseline (LSG)	Shot Peened	LPB Treated
Base (No FOD, No Salt)	✓	✓	✓
Salt Exposure	✓	✓	✓
Simulated FOD	✓	✓	✓
Simulated FOD + Salt Exposure	✓	✓	✓

SCC tests were performed on C-ring specimens (Figure 6) machined from of a 300M steel landing gear. The gage region of the C-ring specimen had a cross section similar to the fatigue specimens shown in Figure 2. The specimen is loaded with a bolt through the 19 mm (0.75 in.) hole, placing the outer surface in nominally uniform tension over the straight gage section. Both untreated and LPB treated specimens were SCC tested at 1033, 1137 and 1240 MPa (150, 165 and 180 ksi) static stress in alternate immersion in a neutral 3.5% NaCl solution. The load was monitored and the time to failure recorded..

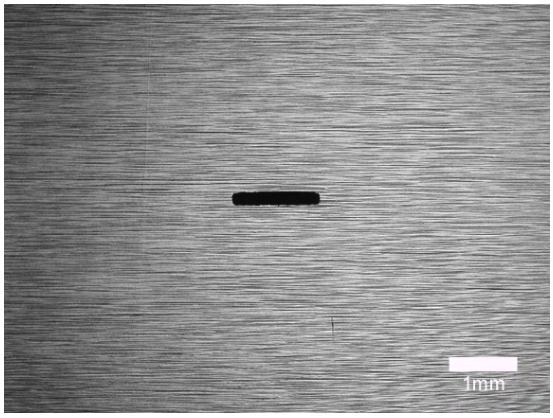

Figure 4a

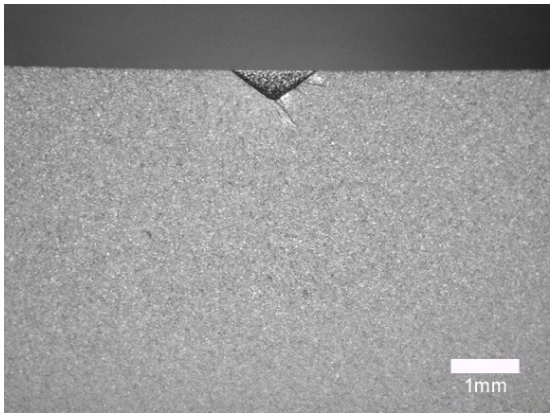

Figure 4b

FIGURE 4 - EDM notch to simulate FOD. (a) Top view, and (b) Cross-section of a 0.020 in. deep notch.

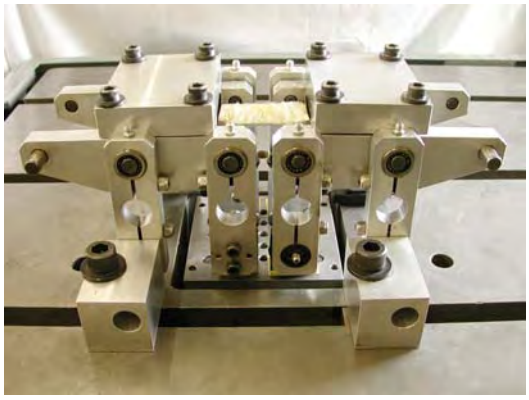

FIGURE 5 - Fatigue test set up.

Fractography

Following fatigue testing, each specimen was examined optically at magnifications up to 60x to identify fatigue origins and locations thereof, relative to the specimen geometry. A few specimens were also examined with SEM.

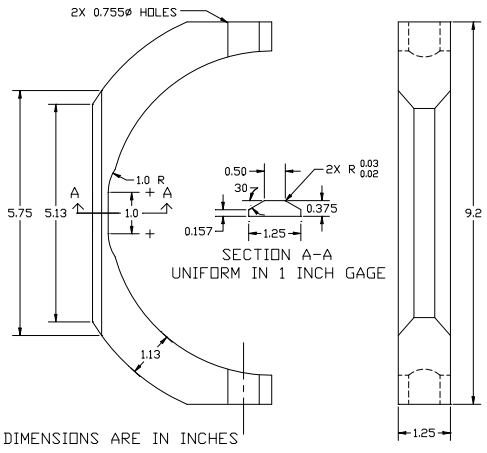

FIGURE 6 - C-ring specimen for SCC tests.

RESULTS AND DISCUSSION

Residual Stress Distributions

The residual stress distributions measured as functions of depth are presented graphically in Figure 7. Compressive stresses are shown as negative values, tensile as positive, in units of ksi (10^3 psi) and MPa (10^6 N/m^2). Compared to SP, LPB produced compressive residual stress of greater magnitude, nominally -1033 MPa (-150 ksi) for SP vs. –1240 MPa (-180 ksi) for LPB with an order of magnitude greater depth. Thermal exposure to 400°F for 48 hrs, simulating baking after electroplating, did not significantly relax the residual stresses from either the SP or LPB treatment.

HCF and Corrosion Fatigue Performance

Figures 8-11 show the HCF and corrosion fatigue performance of 300M steel as maximum stress S-N curves. In Figure 8, the baseline material performance with and without the EDM notch and exposure to the corrosive environment is presented. The unnotched baseline condition has a fatigue strength of nominally 1035 MPa (150 ksi). In the presence of a neutral 3.5% salt solution, the corrosion fatigue strength of baseline condition drops markedly to only 205 MPa (30 ksi). The baseline material exhibited an endurance strength, however the endurance strength is not well defined in the presence of salt solution, indicating further loss of strength with increasing time and cycles. Introduction of a semi-elliptical EDM notch 0.5 mm (0.020 in.) deep drastically decreases the fatigue strength to about 140 MPa (30 ksi) in air, and to less than 70 MPa (10 ksi) in the salt solution. Power law lines were fit to the data in Figure 8, and represent the average behavior of the material in its baseline condition.

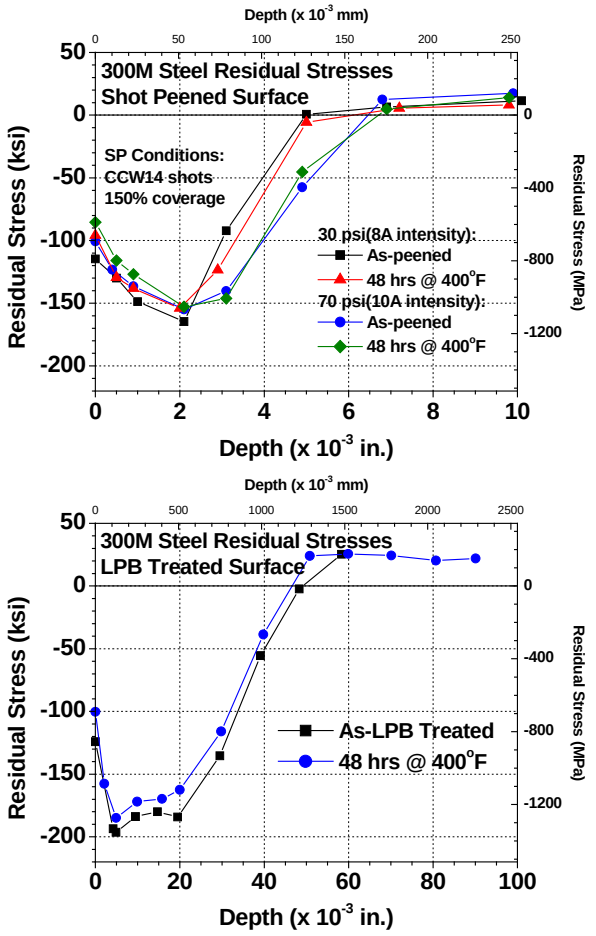

FIGURE 7 - Residual stress distribution for SP and LPB processed specimens. Thermal exposure at 400°F showed no significant effect on residual stresses.

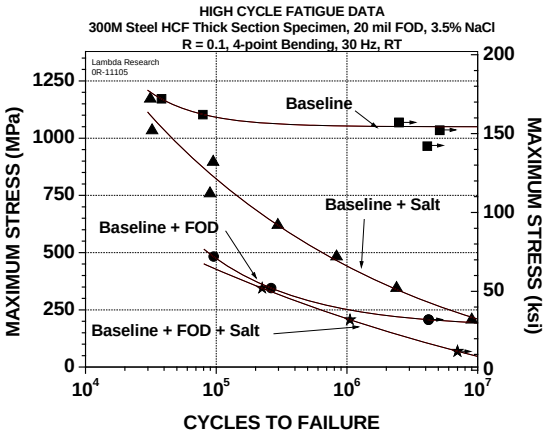

FIGURE 8 - Baseline fatigue results

Figure 9 shows the HCF and corrosion fatigue performance of both unnotched and notched SP treated specimens. Benefits of surface compression from the SP treatment are clearly demonstrated in the improved HCF performance of the unnotched specimens. Corrosion fatigue strength in the presence of the neutral salt environment is reduced to nominally 515 MPa (75 ksi).

This loss of fatigue strength, by a factor of 2, is not as severe as the factor of 5 debit seen in the baseline material. However, the introduction of a 0.5 mm (0.020 in.) deep notch, exceeding the depth of the SP compressive layer, reduces the performance to essentially that of the notched baseline condition both in air and in neutral salt.

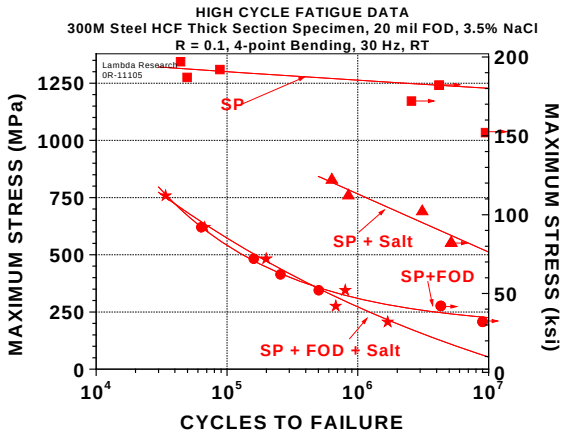

FIGURE 9 - Fatigue results for SP

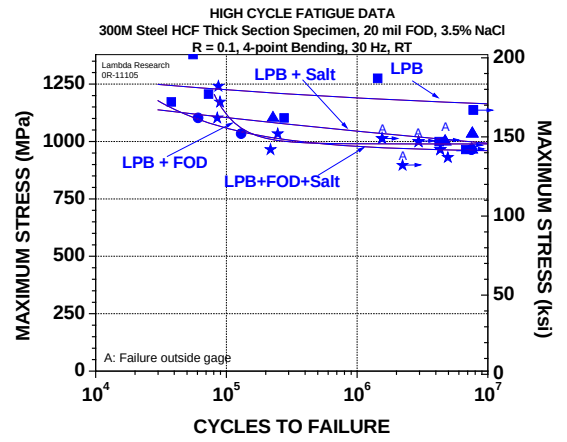

FIGURE 10 - Fatigue results for LPB

Figure 10 shows the HCF and corrosion fatigue behavior of LPB treated specimens. The unnotched specimen shows superior HCF performance, with a fatigue strength of 1200 MPa (175 ksi). Results for notched and unnotched conditions with corrosion indicate a fatigue strength of 1000 MPa (145 ksi), just slightly lower than the baseline material. The LPB process has effectively mitigated corrosion fatigue. The HCF and corrosion fatigue performance of the LPB group is statistically similar to the unnotched baseline material. The endurance limit behavior that was absent in both baseline and SP treatment when tested in the neutral salt solution environment is restored with the LPB treatment, an important finding for legacy aircraft operated at extended lives.

Figure 11 shows a summary of HCF and corrosion fatigue test results. Here, it is evident that a 0.5 mm (0.020 in) deep EDM notch greatly decreases the HCF and corrosion fatigue strength for both baseline and SP conditions. In contrast, the LPB treated specimens withstood the same EDM notch with a fatigue strength of 1000 MPa (145 ksi).

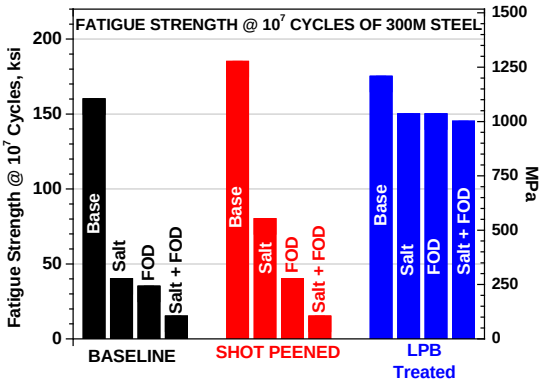

FIGURE 11 – Summary of Fatigue Results

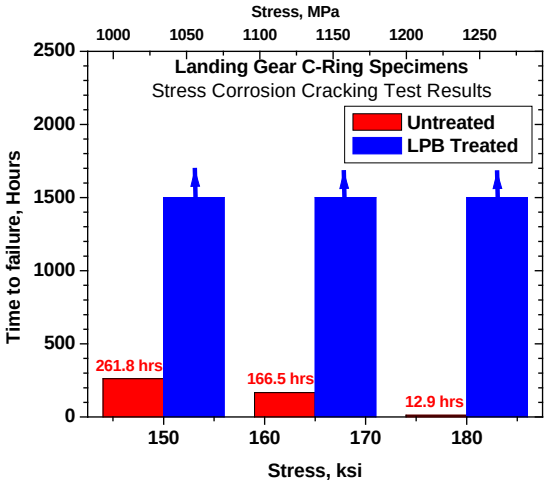

FIGURE 12 - SCC test results.

In Figure 12 the SCC test results show the untreated baseline material had SCC time to failure of 261.8 hrs at 1034 MPa (150 ksi), 166.5 hrs at 1138 MPa (165 ksi) and only 12.9 hrs at 1241 MPa (180 ksi), respectively. The LPB treated specimens did not fail even after 1500 hrs. of exposure at all three stress levels. When the specimens were loaded to higher stress levels the specimens were permanently bent with still no cracking from SCC. These results indicate the deep surface compressive stresses from LPB prevent the surface in contact with the corrosive environment from ever reaching the SCC threshold stress, thus fully mitigating SCC as a failure mechanism in 300M.

Fractography

Fractographic analyses presented in Figures 13, 14 and 15 are limited to baseline, SP and LPB unnotched corrosion fatigue tested specimens. Fractographic analyses of the notched and other HCF test conditions yielded results that are expected and consistent with the fatigue test results shown in Figures 8-11, and therefore are not further described.

Figure 13a shows the fracture surface of a baseline specimen with a single crack initiation site near the corner of the trapezoidal cross-section. Figures 13b and c show the role of corrosion pits on the crack initiation process. Similarly Figures 14a, b and c, and Figures 15a, b, c and d show the optical fractographs, the gage of surface with corrosion pits, and the cross-sectional view of a corrosion pit in an unnotched SP and LPB specimen. In all cases, pitting of the gage surface is evident, and the cross-sectional views indicate a gradual increase in the depth of corrosion pitting damage with increased time of testing. In both baseline and SP specimens, the corrosion pits resulted in early crack initiation at low stresses, leading to final failure. In contrast, for LPB specimens, despite the higher stress levels and deeper corrosion pitting damage due to the longer exposure time during testing, the corrosion fatigue performance is minimally affected. This is seen in Figures 15a and b, where subsurface crack initiation is evident despite the presence of deep corrosion pits similar to the one seen in the cross-sectional view in Figure 15d.

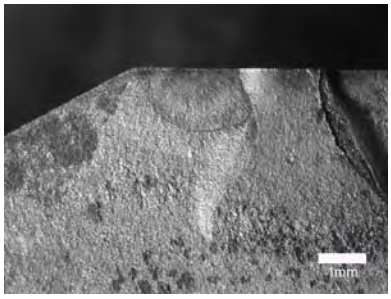

FIGURE 13a

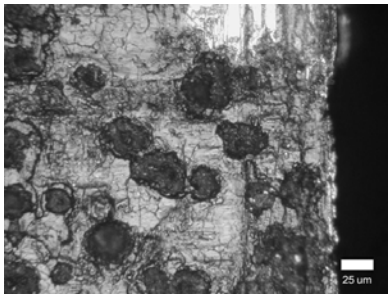

FIGURE 13b

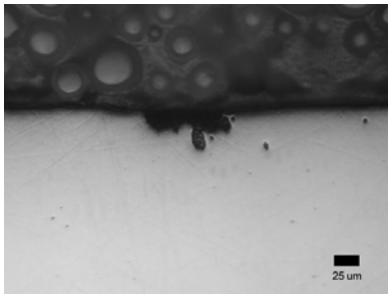

FIGURE 13c

FIGURE 13 - (a) Fracture surface showing crack initiation (arrow) from a corrosion pit, (b) gage surface of the specimen showing a typical set of corrosion pits, and (c) cross-sectional view of a typical corrosion pit in a corrosion fatigue tested baseline specimen; S/N 97, Smax=50 ksi, Nf=2.4(10^6) cycles (~24 hours)

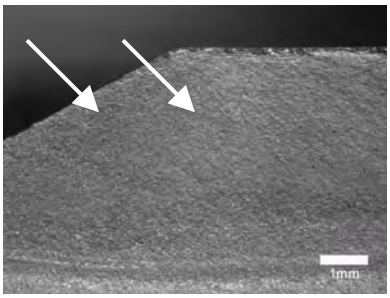

FIGURE 14A

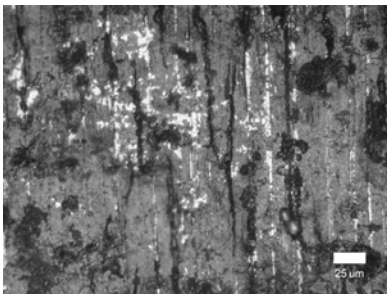

FIGURE 14b

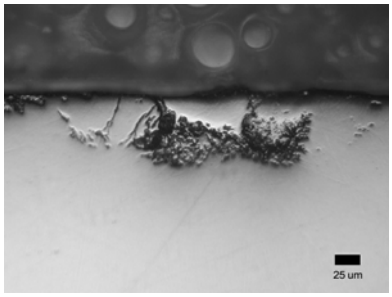

FIGURE 14c

FIGURE 14 - (a) Fracture surface showing multiple crack initiation (arrows) sites, (b) gage surface showing a set of typical corrosion pits, and (c) cross-sectional view of a typical corrosion pit in a corrosion fatigue tested SP specimen; S/N 94, Smax=100 ksi, Nf=3.1(10^6) cycles (~30 hours).

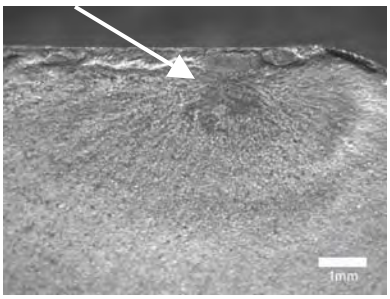

FIGURE 15a

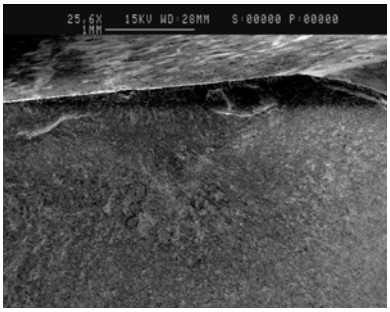

FIGURE 15b

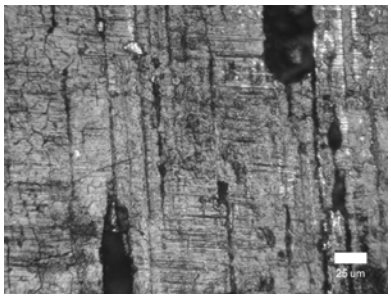

FIGURE 15c

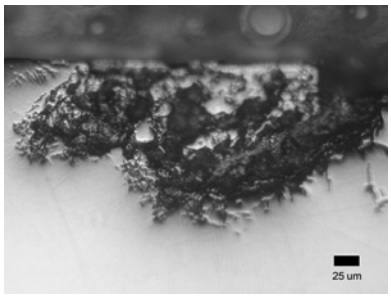

FIGURE 15d

FIGURE 15 - (a) Optical fractograph showing subsurface crack initiation (arrow) site, (b) SEM fractograph showing the same region, (c) gage surface corrosion pits and cracking, and (c) cross-sectional view of a typical corrosion pit in a corrosion fatigue tested LPB specimen; L/N 11, Smax=150 ksi, Nf=7.1(10^6) cycles (~70 hours)

CONCLUSION

The fatigue, salt-water corrosion fatigue, and FOD tolerance of LPB, shot peened and as-machined 300M steel was compared. LPB provided a compressive layer an order of magnitude deeper and more compressive than 8-10A shot peening. LPB completely mitigated the fatigue debits from both 0.5 mm deep FOD and salt-water exposure, providing fatigue strength and life comparable to undamaged baseline material. Shot peening provided only half of the salt-water corrosion fatigue strength of LPB. The results overwhelmingly indicate that the deep surface compression from LPB completely mitigated alternate immersion salt water SCC under static stress up to at least 75% of the yield strength of the alloy.

ACKNOWLEDGMENTS

Support of this work by IR&D funds from Lambda Technologies and the Air Force Material Laboratory is gratefully acknowledged. The authors also wish to thank Tom Lachtrupp for residual stress measurements; Perry Mason for conducting fatigue tests, and Brian Tent for SEM analysis.

REFERENCES

1. E. U. Lee, C. Lei, H.C. Sanders, R. Taylor, (2004), "Evolution of Fractograph During Fatigue and Stress Corrosion Cracking," Naval Air Warfare Center, Aircraft Div Patuxent River Md, Report Number(S)-NAWCADPAX/TR-2004/12 Unclassified report.
2. E. U. Lee, (1995), Metall. Mater. Trans. A, 26A, (5); May, pp. 1313-1316.
3. Eun U. Lee, "Corrosion Behavior of Landing Gear Steels," Naval Air Warfare Center Aircraft Div Warminster Pa Air Vehicle And Crew Syst Ems Technology Dept, Report Number - NAWCADWAR-94001-60 Unclassified report.
4. "High-Strength Steel Joint Test Protocol for Validation of Alternatives to Low Hydrogen Embrittlement Cadmium For High-Strength Steel Landing Gear and Component Applications", (2003), July 31, Prepared by: The Boeing Company, Phantom Works, Seattle, Washington 98124, and Concurrent Technologies Corporation *(CTC)* Contract #CTC/LAU-CL2402-02 For: Air Force Research Laboratory Task Order 5TS5702D035M.
5. ASM Handbook, Vol. 19, Fatigue and Fracture, S.R. Lampman, ed., ASM International, Metals Park, OH, 1996, pp. 596-597.
6. Frost, N.E. Marsh, K.J. Pook, L.P., (1974), *Metal Fatigue*, Oxford University Press.
7. Fuchs, H.O. and Stephens, R.I., (1980), *Metal Fatigue In Engineering*, John Wiley & Sons.
8. Berns, H. and Weber, L., (1984), "Influence of Residual Stresses on Crack Growth," Impact Surface Treatment, edited by S.A. Meguid, Elsevier, 33-44.
9. Ferreira, J.A.M., Boorrego, L.F.P., and Costa, J.D.M., (1996), "Effects of Surface Treatments on the Fatigue of Notched Bend Specimens," Fatigue, Fract. Engng. Mater., Struct., Vol. 19 No.1, pp 111-117.
10. Prevéy, P.S. Telesman, J. Gabb, T. and Kantzos, P., (2000), "FOD Resistance and Fatigue Crack Arrest in Low Plasticity Burnished IN718," Proc of the 5th National High Cycle Fatigue Conference, Chandler, AZ. March 7-9.
11. Clauer, A.H., (1996), "Laser Shock Peening for Fatigue Resistance," Surface Performance of Titanium, J.K. Gregory, et al, Editors, TMS Warrendale, PA, pp 217-230.
12. T. Watanabe, K. Hattori, et al,, (2002), "Effect of Ultrasonic Shot Peening on Fatigue Strength of High Strength Steel," Proc. ICSP8, Garmisch-Partenkirchen, Germany, Ed. L. Wagner, pg 305-310.
13. P. Prevéy, N. Jayaraman, R. Ravindranath, (2003), "Effect of Surface Treatments on HCF Performance and FOD Tolerance of a Ti-6Al-4V Vane," Proceedings 8th National Turbine Engine HCF Conference, Monterey, CA, April 14-16.
14. Paul S. Prevéy, Doug Hornbach, Terry Jacobs, and Ravi Ravindranath, (2002), "Improved Damage Tolerance in Titanium Alloy Fan Blades with Low Plasticity Burnishing," Proceedings of the ASM IFHTSE Conference, Columbus, OH, Oct. 7-10.
15. Paul S. Prevéy, et. al., (2001), "The Effect of Low Plasticity Burnishing (LPB) on the HCF Performance and FOD Resistance of Ti-6Al-4V," Proceedings: 6th National Turbine Engine High Cycle Fatigue (HCF) Conference, Jacksonville, FL, March 5-8.
16. M. Shepard, P. Prevéy, N. Jayaraman, (2003), "Effect of Surface Treatments on Fretting Fatigue Performance of Ti-6Al-4V," Proceedings 8th National Turbine Engine HCF Conference, Monterey, CA, April 14-16.
17. Paul S. Prevéy and John T. Cammett, (2002), "Restoring Fatigue Performance of Corrosion Damaged AA7075-T6 and Fretting in 4340 Steel with Low Plasticity Burnishing," Proceedings 6th Joint FAA/DoD/NASA Aging Aircraft Conference, San Francisco, CA, Sept 16-19.

18. N. Jayaraman, Paul S. Prevéy, Murray Mahoney, (2003), "Fatigue Life Improvement of an Aluminum Alloy FSW with Low Plasticity Burnishing," Proceedings 132nd TMS Annual Meeting, San Diego, CA, Mar. 2-6.
19. Paul S. Prevéy and John T. Cammett, (2002), "The Influence of Surface Enhancement by Low Plasticity Burnishing on the Corrosion Fatigue Performance of AA7075-T6," Proceedings 5th International Aircraft Corrosion Workshop, Solomons, Maryland, Aug. 20-23.
20. John T. Cammett and Paul S. Prevéy, (2003), "Fatigue Strength Restoration in Corrosion Pitted 4340 Alloy Steel Via Low Plasticity Burnishing" Retrieved from www.lambda-research.com Sept. 5.
21. Paul S. Prevéy, (2000), "Low Cost Corrosion Damage Mitigation and Improved Fatigue Performance of Low Plasticity Burnished 7075-T6," Proceedings of the 4th International Aircraft Corrosion Workshop, Solomons, MD, Aug. 22-25.
22. Hilley, M.E. ed.,(2003), Residual Stress Measurement by X-Ray Diffraction, HS*J784*, (Warrendale, PA: SAE).
23. Noyan, I.C. and Cohen, J.B., (1987) Residual Stress Measurement by Diffraction and Interpretation, (New York, NY: Springer-Verlag).
24. Cullity, B.D., (1978) Elements of X-ray Diffraction, 2nd ed., (Reading, MA: Addison-Wesley), pp. 447-476.
25. Prevéy, P.S., (1986), "X-Ray Diffraction Residual Stress Techniques," *Metals Handbook*, **10**, (Metals Park, OH: ASM), pp 380-392.
26. Koistinen, D.P. and Marburger, R.E., (1964), Transactions of the ASM, **67**.
27. Moore, M.G. and Evans, W.P., (1958) "Mathematical Correction for Stress in Removed Layers in X-Ray Diffraction Residual Stress Analysis," SAE Transactions, **66**, pp. 340-345.